Mineralogical and chemical characteristics of the lead-zinc tailing and contaminated soil from the mine tailing pond in Hunan Province (China)

Chuanchang Li[*], Ling Zeng[**], Hongyuan Fu[**], Jian Chen[*], Jianjun He[*], Zhongming He[***]

[*] School of Energy and Power Engineering, Changsha University of Science and Technology, Changsha 410114, China. Corresponding author: chuanchangli@csust.edu.cn (Chuanchang Li)

[**] School of Civil Engineering and Architecture, Changsha University of Science and Technology, Changsha 410114, China, zlbingqing3@126.com (Ling Zeng)

[***] School of Traffic and Transportation Engineering, Changsha University of Science and Technology, Changsha 410014, China

Abstract: The mineralogical and chemical characteristics of heavy metals in tailings and soils is an imperative for potential ecological risk assessment of metals to environment and heavy metals pollution prevention and control. The lead-zinc tailing and contaminated soil in and near the tailing pond were sampeled from a mine tailing pond in Hunan province (China), in which the chemical composition, phase composition and thermal behavior of tailing and soil were investigated. Furthermore, the petrography of lead-zinc tailing and chemical fractionations of Pb and Zn in the contaminated soil were studied in details. The mineral phases of lead-zinc tailing were galena, pyrite, chalcopyrite, sphalerite, quartz and fluorite, as distinguished by the reflected light microscopy and further proofed by the scanning electron microscope-energy dispersive spectrometer under the back scattered electron mode. Chemical fractionations were carried out by the European Community Bureau of Reference (BCR) sequential extraction procedure for Pb and Zn in the soil and the mild acido-soluble (F1), reducible (F2), oxidizable (F3), and residual (F4) fractions were 5.90, 75.24, 4.90 and 13.96% for Pb, and 47.74, 34.06, 9.59 and 8.61% for Zn, respectively. Subsequently, the individual contamination factor (*ICF*) of Pb and Zn were calculated as 6.16 and 10.61, respectively. The DTPA-available content of Pb and Zn in the contaminated soil were 39.9 and 170.7 mg·kg^{-1}, respectively. The study provided a base for selecting remediation strategies in the studied area.

Keywords: mineralogical characteristics, chemical fractionations, remediation

Introduction

Metals and their alloys are main basic raw materials in a variety of domains. Metallic minerals are the main resources for the metals. Flotation is the widely used method to extract metallic minerals from the coexisting gangue minerals in ore deposit (Gao et

al., 2016a; Gao et al., 2016b; Wang et al., 2016). However, abundant of flotation tailings are generated from flotation processing. The disposal of tailings, which usually consists of sand, pyrite, residual metal sulfides and reagents, gradually creates huge environmental problems if the tailings pond is not properly rehabilitated (Antonijevic et al., 2012; Zheng et al., 2015; González-Valdez et al., 2016). This presents a problem for many mines in the world, the active and abandoned mine sites alike. Mine tailings ponds are environmental hazards because the tailing is easily leached and eroded by water, which could cause a true environmental disaster including pond failure and contaminated surrounding soil (Antonijevic et al., 2012; Wang and Liang, 2015; Ciszewski and Grygar, 2016). The ecology and health of people surrounding the tailing pond area are under serious threat, and long term hidden danger is heavy metal that eroded from the heavy metal tailing by rainwater (Su et al., 2014). The heavy metals in water tend to precipitate rapidly or to be adsorbed onto solid particles (Ciszewski and Grygar, 2016). Also, rainwater irrigation may lead to the storage of heavy metals in agricultural soils and plants (Amin and Ahmad, 2015), and may be hazardous to animal and human health through the food chains (Shi et al., 2014). Due to the high risk on human health and ecological security, contaminated soils need to be remediated for their reclamation (Mao et al., 2015).

Over the last several decades, physical, chemical and biological approaches have been used to remediate heavy metals contaminated soils (Mahar et al., 2016), including in situ stabilization of heavy metals using mineral amendments (Floris et al., 2017), phytoremediation (Mahar et al., 2016), electrochemical remediation (Yeung and Gu, 2011; Ren et al., 2014) and thermal treatments (Akcil et al., 2015). The element and chemical fractionations of heavy metals must be acquired before mineral remediation, on account of mineral amendments are targeted to stabilize the specific heavy metal element (Floris et al., 2017). Because of only a portion of soil metal is bioavailable for uptake by plants (Ali et al., 2013), the content of metal available to plants should be obtained for phytoremediation (Chojnacka et al., 2005). Also thermal behavior of soil should be gained for thermal treatments (Akcil et al., 2015). The above mentioned are belong to mineralogy and chemistry of soil. Otherwise, to comprehensive remediate contaminated soils surrounding the tailings pond, the tailing in the pond also need to be appropriately disposed in mineralogy of tailing should be uncovered before remediation.

Therefore, revealing the mineralogical and chemical characteristics of the tailing and soil are effective for selecting remediation strategies. A lead-zinc mine and its tailings pond in Hunan Province (China) have an over 50-year history (Lei et al., 2015). However, there are few reports about the research on the mineralogical and chemical characteristics of tailing and soil of this pond. In this paper the mineralogical and chemical studies of tailing and soil of this site is conducted with the purpose of selecting appropriate strategies for remediation of the contaminated soil.

Experimental

The lead-zinc tailing was sampled from the tailing pond of a lead-zinc mine in Hunan, China (Fig. 1), and contaminated soil was collected from the upper 30 cm layer of cultivated land, which is close to the pond. We sampled soil from four cultivated land and then pooled the samples for further use. After being transported to the laboratory, these soil samples were air-dried, ground to pass through a 1 mm plastic sieve, homogenized and stored in polypropylene plastic sample bag.

Fig. 1. Map of sampling area located in Hunan Province

An elemental composition of lead-zinc tailing and contaminated soil was determined by X-ray fluorescence (XRF) using radiation at an acceleration voltage of 100 kV and current of 80 mA (PANalytical Epsilon 5). X-ray diffraction (XRD) was carried out using a Rigaku D/max-rA analyzer (Cu-Kα) under the following conditions: voltage 40 kV, current 250 mA, scan range from 5 to 80° and step size of 0.02°. The crystalline phases of samples were identified using the software Jade 5.0 compiled by Materials Data Inc (MDI). The lead-zinc tailing was embedded in the epoxy resin and polished for the petrography analysis, the photomicrographs were then obtained using a Leica DFC480 photomicroscope. The samples were pressed onto a conductive adhesive tab which mounted on a copper stub and coating with gold before the test, and the corresponding microstructures were investigated using a FEI Quanta-200 scanning electron microscope (SEM) operated at an accelerating voltage at 20 kV. Fourier transformation infrared spectroscopy (FTIR) spectra were recorded using a Thermo Electron Corporation Nicolet Nexus 670 FTIR spectrometer in the range of 4000~400 cm^{-1}. TGA (weight loss curve and deriv. weight) analyses were conducted at a heating rate of 10 °C·min^{-1} up to 1000 °C in nitrogen atmosphere, using α-Al$_2$O$_3$ crucibles in SDT Q600 equipment from TA Instruments-Waters LLC, USA.

The sequential extraction was carried out according to the European Community Bureau of Reference BCR sequential extraction procedure (Fathollahzadeh et al., 2014). The method determined four well defined geochemical fractions of metals in contaminated soil: mild acido-soluble (F1), reducible (F2), oxidizable (F3) and residual (F4) fractions. All reagents used to perform extraction were of analytical grade. A detailed description of fractionation procedures was given as follows.

Step 1 (mild acido-soluble fraction): the first fraction of metals was extracted by accurately weighing 1.0 g of contaminated soil, placing in a polyethylene centrifuge cup (250 cm^3) followed by the addition of 40 cm^3 of 0.11 M acetic acid and mechanically shaken (200 rpm) on an end-over-end shaker for 16 h at room temperature. The extract was then separated from the residue by centrifugation at 3000 g for 20 min, stored in the polypropylene tubes and labeled as L1 for further analysis. To continue in Step 2, the residual soil was washed with 20 cm^3 distilled water, shaken for 15 min, and centrifuged at 3000 g for 20 min. In a sequence, decantation of supernatant was carried out to eliminate any remaining particles before the next extraction step, and residue was labeled as R1.

Step 2 (reducible fraction): 40 cm^3 of fresh hydroxyl ammonium chloride 0.5 M was added to the R1 and shaken (200 rpm) for 16 h at room temperature. Extraction was performed as previously described in Step 1, and the extract and residue were labeled as L2 and R2, respectively.

Step 3 (oxidizable fraction): The first digestion, 10 cm^3 of hydrogen peroxide (30%) adjusted to pH 2–3 with nitric acid was carefully added to R2 in a centrifuge cup and covered for digesting at room temperature for 1 h and at 85 ± 2 °C in a water bath for additional 1 h, and manual shook every ten minutes. Then, it was uncovered and heated at 85 ± 2 °C until the final volume was less than 3 cm^3. Samples were then removed from the water bath, cooled down to room temperature. Following the digestion, a second addition of 10 cm^3 pH-adjusted hydrogen peroxide was carried out as previously described in the first digestion, and then uncovered and heated at 85 ± 2 °C until the final volume was less than 1 cm^3. Samples were then removed from the water bath, cooled down to room temperature followed by addition of 50 cm^3 of 1.0 M ammonium acetate and shook for 16 h. The extraction was performed as previously described in the Step 1, and the extract and residue were labeled as L3 and R3, respectively.

Step 4 (residual fraction): the residue (R3) was placed in the centrifuge cup and heated at 60 °C until evaporate to dryness. Then, it was weighed 1.0 g of dry R3, and dissolved with a mixture of hydrochloric acid, nitric acid, hydrofluoric acid and perchloric acid.

Water-soluble fraction (F0): 1.0 g of contaminated soil was weighed and placed in the polyethylene centrifuge cup (250 cm^3), and followed by the addition of 20 cm^3 of cooled down boiled water (pH 7.0) and mechanically shook (200 rpm) on an end-over-end shaker for 16 h at room temperature. The extract was then separated from the

residue by centrifugation at 4500 g for 30 min, stored in the polypropylene tubes and filtrated through a 0.45-μm membrane for further analysis.

Prior to the analysis, all extracts were stored in the refrigerator at 4 °C. The analysis of Pb and Zn contents was performed with an ICP-MS (NexION 300X, Perkin Elmer). The pH of lead-zinc tailing and contaminated soil were measured in a 1/2.5 (w/v) suspension of samples in CO_2-free deionized water using laboratory scale pH meter (PHS-3C Model), and the pH of lead-zinc tailing and contaminated soil were 6.67 and 6.55.

The content of Pb and Zn was determined according to a method of Lindsay and Norvell (1978) by extraction with DTPA. The extractant consisted of 0.005M DTPA (diethylenetriaminepentaacetic acid), 0.1M triethanolamine, and 0.01M $CaCl_2$, with a pH of 7.3. The soil test consisted of shaking 5 g of air-dry soil with 20 cm^3 of extractant for 2 hours. The leachate was filtered, and Pb and Zn were measured in the filtrate by using a graphite furnace atomic absorption spectrophotometer (Hitachi High-Tech, ZA3700).

Results and discussion

Table 1 presents the results of XRF testing. The contents of Zn and Pb were 0.191 wt.% and 0.044 wt.% for lead-zinc tailing, respectively, while 0.190 wt.% and 0.031 wt.% for soil. It indicated that the soil maybe contaminated by the lead-zinc tailing. Figure 2 shows XRD patterns of the lead-zinc tailing and contaminated soil, indicating the respective phase composition such as quartz, fluorite, muscovite, kaolinite and franklinfurnaceite. The major phase of the lead-zinc tailing and contaminated soil was quartz. The muscovite, kaolinite and franklinfurnaceite appeared in two samples. It was indicated that the contaminated soil had homology with lead-zinc tailing. Four reflections at 2θ = 28.22°, 246.96°, 55.68°, and 75.85° were identified as fluorite, which only appeared in the lead-zinc tailing. From the semiquantitative results of the XRD analysis, the mineralogical compositions were quartz (78.3 wt.%), fluorite (6.1 wt.%), muscovite (5.2 wt.%), kaolinite (5.3 wt.%) and franklinfurnaceite (5.1 wt.%) for the lead-zinc tailing, and quartz (77.2 wt.%), muscovite (8.1 wt.%), kaolinite (9.7 wt.%) and franklinfurnaceite (5.0 wt.%) for the contaminated soil. These results were in accord with the XRF results.

The FTIR spectra of lead-zinc tailing and contaminated soil are shown in Fig. 3. The band at 3620 cm^{-1} in the contaminated soil was assigned to the hydroxyl-stretching modes of inner hydroxyl groups. The absorption at 3420 cm^{-1} in all samples was attributed to loosely bound water (v(H-O-H)) (Li et al., 2013), and the absorption band at 1626 cm^{-1} was induced by O–H stretching from adsorbed water (Ruan et al., 2001). The band at 1382 cm^{-1} in all samples was attributed to symmetric stretching vibration from adsorbed CO_2. The bands at 1106 cm^{-1} in lead-zinc tailing and 1028 cm^{-1} in the contaminated soil were assigned to apical Si–O stretching and skeleton Si–O–Si stretching, respectively (Hu and Yang, 2013). The bands at 784 cm^{-1} and 694

cm^{-1} in the samples were attributed to Al–OH translational vibration (Li et al., 2015). The bands at 617 cm^{-1} in the samples was induced by O–Al–O bending vibration (Voll et al., 2002). The band at 527 cm^{-1} in the contaminated soil was attributed to Si–O–Al^{VI} bending (Li et al., 2015), while a feeble absorption band in the lead-zinc tailing. The band at 463 cm^{-1} in the samples was attributed to Si–O bending (Li et al., 2015).

Table 1. XRF results of samples (wt.%)

|	O	F	Na	Mg	Al	Si	P	S
lead-zinc tailing	49.922	2.210	0.210	0.200	2.195	38.107	0.028	0.141
contaminated soil	49.640	0.256	0.171	0.461	8.160	34.709	0.048	0.272
	Cl	K	Ca	Ti	Cr	Mn	Fe	Cu
lead-zinc tailing	0.024	0.912	4.353	0.121	0.010	0.031	1.215	0.015
contaminated soil	0.014	1.817	0.651	0.491	0.007	0.079	2.896	0.011
	Zn	Ga	Rb	Sr	Zr	Ba	Pb	Ni
lead-zinc tailing	0.191	0.001	0.007	0.006	0.003	0.044	0.044	--
contaminated soil	0.190	0.002	0.010	0.010	0.025	0.044	0.031	0.004
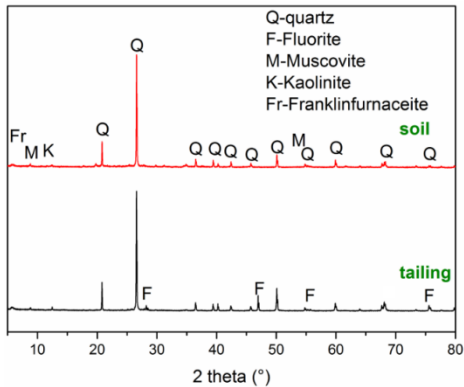
Fig. 2. XRD patterns of the lead-zinc tailing and contaminated soil
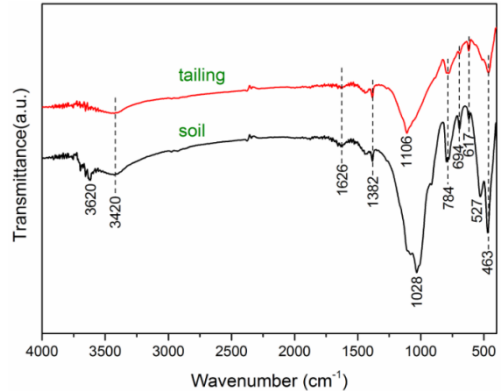

Fig. 3. FTIR spectra of the lead-zinc tailing and contaminated soil

The derivative of the weight loss (DTG) and TG curves of lead-zinc tailing under the flow of N_2 are shown in Fig. 4a. According to the TG curve, free water was released in the temperature internal 40–100 °C with the mass loss of 0.20%, and the DTG curve showed that the weight loss reached maximum at 80 °C in this stage. Dehydration of lattice water occurred in 100–436 °C with the mass loss of 1.48%, and the weight loss reached maximum at 147 °C in this temperature range. From 436 °C to 1000 °C, the weight loss kept the rising trend with the mass loss of 5.35% due to the removal of the structural hydroxyls. Figure 4b shows the derivative of the weight loss (DTG) and TG curves of the contaminated soil under the flow of N_2. According to the

TG curve, free water was released in the temperature internal 40–130 °C with the mass loss of 0.85%, and the DTG curve showed that the weight loss reached maximum at 105 °C. The lattice water and structural hydroxyls (part) were released in 130–676 °C with the mass loss of 5.90%, and the weight loss reached maximum at 490 °C in this stage. From 676 to 1000 °C, the weight loss was relatively stable with the mass loss of 4.20%, and structural hydroxyls were removed. There were no obvious chemical reactions under N_2 atmosphere at room temperature to 1000 °C. It indicated that the lead-zinc tailing and contaminated soil had a good thermal stability.
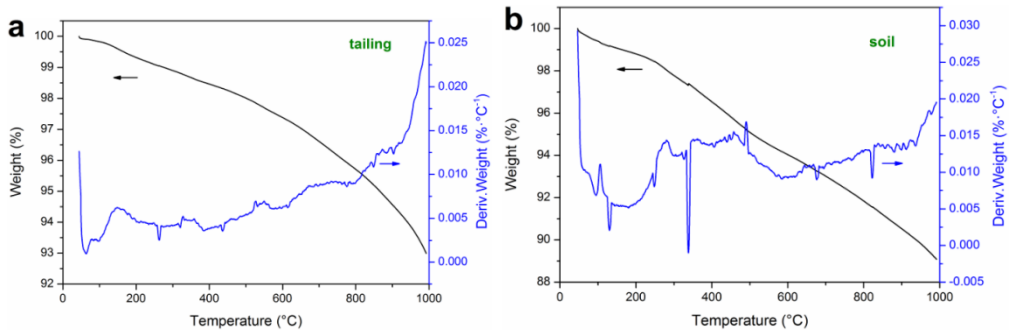

Fig. 4. TGA (weight loss curve and derivative weight) curves of lead-zinc tailing (a) and contaminated soil (b) in nitrogen atmosphere

The petrography study is useful for identification of rocks, minerals and ores (Xu et al., 1992; Li et al., 2013). The reflected light microscopy images demonstrated that five types of mineral phases were easily distinguished in the lead-zinc tailing (Fig. 5). The irregular galena particles (20-30 μm) were surrounded by quartz (Fig. 5a), and minor pyrite and sphalerite were embedded in galena (Fig. 5b). Fluorite was distributed in quartz in a wide range of sizes (Fig. 5c), and chalcopyrite was continuous (Fig. 5c) or dispersive (Fig. 5d) implanted in quartz. Also, it existed uniparted pyrite, galena and sphalerite in the sample (Fig. 5e and Fig. 5f). Therefore, the mineralography composition of lead-zinc tailing were coarse-grained galena, minor pyrite and chalcopyrite partially replacing host quartz, with sphalerite distributing in the quartz. Galena and sphalerite may be the heavy metal sources of the contaminated soil, basing on surface broken bonds property of galena and sphalerite (Gao et al., 2014; Gao et al., 2017).

SEM-EDS of the polished lead-zinc tailing sample under the back scattered electron (BSE) mode is presented in Fig. 6, and atomic composition contrasts (Z-contrast) are also identified. Four different contrasts existed in Fig. 6a and were labeled as A1, A2, A3, and A4, respectively. According to EDS results (Fig. 6b), the A1, A2, A3, and A4 were quartz, galena, pyrite hybrid sphalerite and fluorite, respectively. It indicated that galena, pyrite, sphalerite and fluorite were embedded in the quartz matrix, and fractional galena was surrounded by fluorite. Three different contrasts (C1, C2 and C3) existed in Fig. 6c and were identified as quartz, galena and

fluorite (Fig. 6d), respectively. The especial regions (E2 and E3) in Fig. 6e were detected by EDS (Fig. 6f) and were identified as barium sulfate and chalcopyrite, respectively. It demonstrated that the barium sulfate particle existed on its own and chalcopyrite was symbiotic with quartz, corresponding with the petrography results. SE images and EDS elemental maps of the contaminated soil are shown in Fig. 7, indicating Si, Al, and K appeared in the concentrated distribution and Pb and Zn presented the uniform distribution. Si mainly originated from quartz Al and K were from aluminosilicate (kaolinite and muscovite). Pb and Zn did not exist as mineral forms (like galena and sphalerite in the lead-zinc tailing), so they may be originated from the lead-zinc tailing.
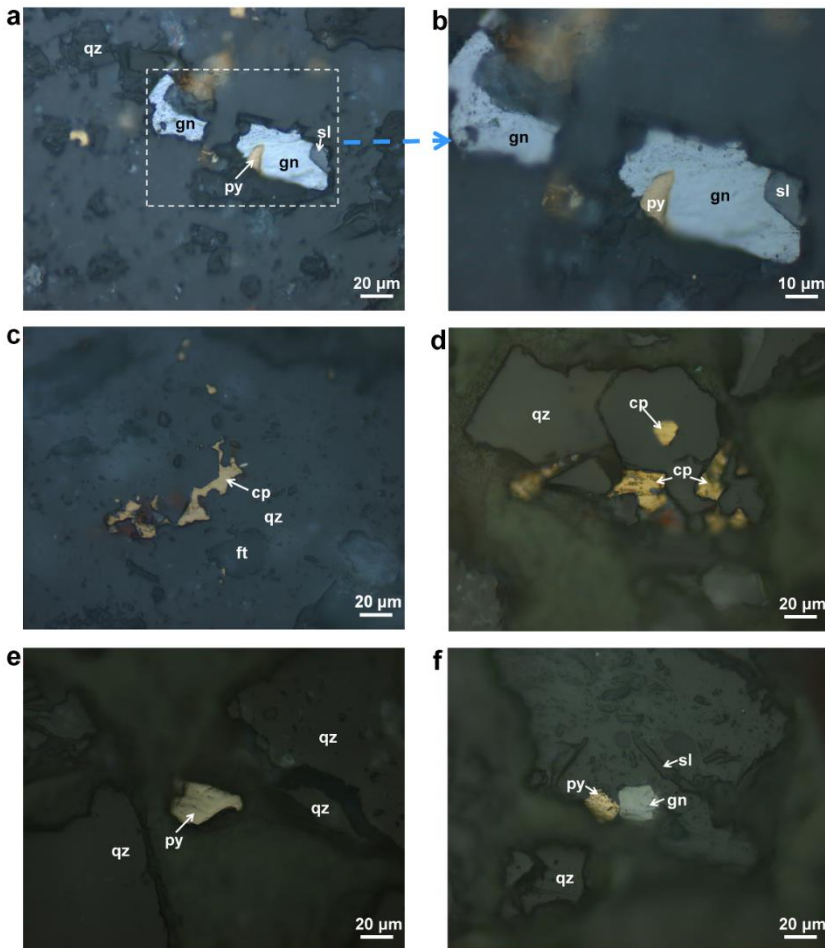

Fig. 5. Reflected light microscopy images of lead-zinc tailing (Abbreviations: gn = galena, py = pyrite, cp = chalcopyrite, sl = sphalerite, qz = quartz, ft = fluorite)
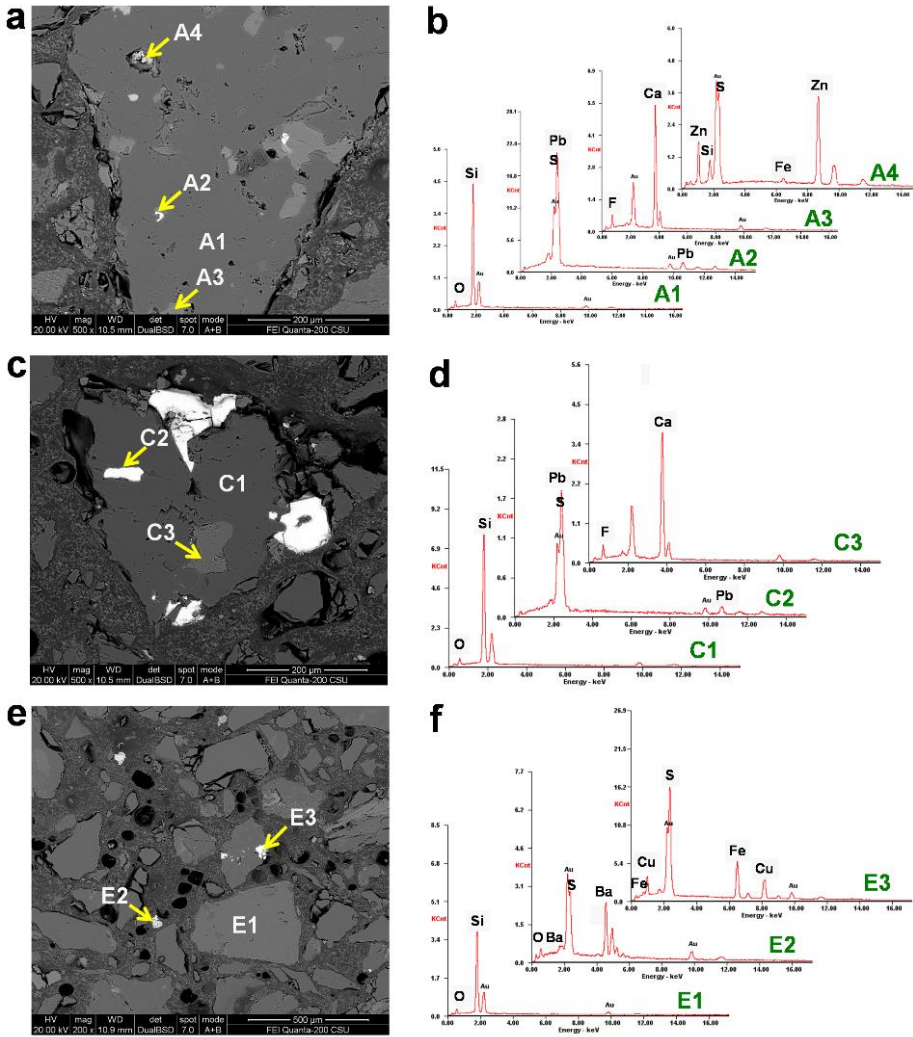
Fig.6. Backscattered electron z-contrast (BSE-Z) images and energy dispersive
X-ray spectroscopic (EDS) of lead-zinc tailing

The elemental fractionation analysis is one of the important contents for eco-geochemical investigation and evaluation (Chai et al., 2015). The investigation of chemical fractionations of heavy metals in soils can provide some valuable information about the potential mobility, bioavailability as well as possible origins. Therefore, the distribution of Pb and Zn in four different fractions in the contaminated soil was investigated (Table 2): mild acido-soluble (F1), reducible (F2), oxidizable (F3) and residual (F4) fractions. Each chemical fraction was presented as the percentage of the sum of all the fractions, and the results are showed in Fig. 8.
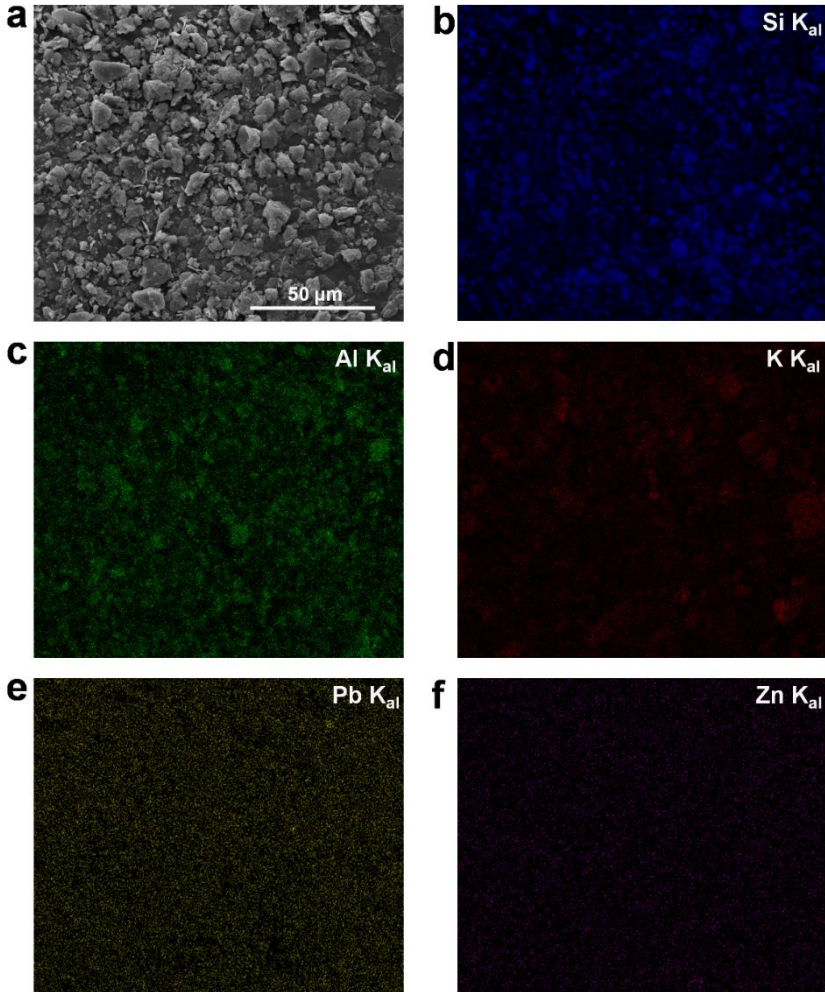
Fig. 7. Secondary electron (SE) images and energy dispersive
X-ray spectroscopic (EDS) elemental maps of contaminated soil

Table 2. Speciation analysis results of contaminated soil (mg·kg^{-1})

Element	Mild acido-soluble fraction	Reducible fraction	Oxidisable fraction	Residual fraction	Available content
Pb	9.34	119.1	7.76	22.1	39.9
Zn	426.3	304.1	85.6	76.9	170.7

The mild acido-soluble fraction (F1) of metals that is adsorbed by interaction of static electricity on the soil particle surface, can be released by ion exchange and weakly associated to carbonates (Fathollahzadeh et al., 2014). Among the four

fractions of heavy metals, the mild acido-soluble fraction may be considered as the mobile and potentially bioavailable ones for either plant or organisms (Chai et al., 2015). The results showed that Pb and Zn were associated with mild acido-soluble fraction with 5.9% and 47.74% of their total concentrations, respectively (Fig. 8), raising concerns due to potential ecological risks mainly in relation to Pb due to its well-known toxic effects to organisms.
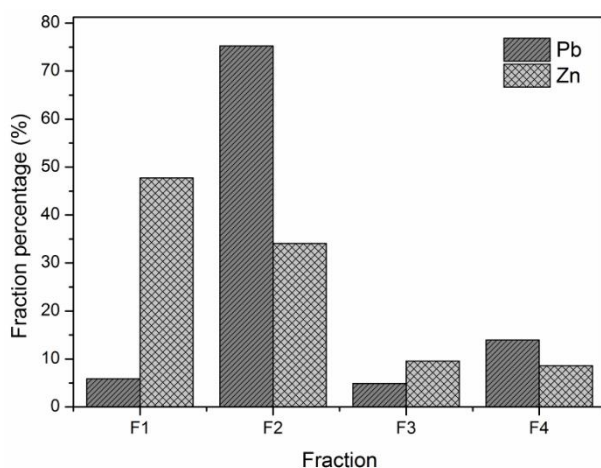

Fig. 8. Chemical fractionation of heavy metals in contaminated soil. (F1, F2, F3 and F4 represent mild acido-soluble, reducible, oxidizable and residual fractions, respectively)

The reducible fraction (F2), indicates the elemental speciation that is usually associated with Fe and Mn oxy/hydroxides (Fathollahzadeh et al., 2014). Pb and Zn were partitioned 75.24% and 34.06% in the reducible fraction, respectively (Fig. 8). The large number of Pb (119.1 mg·kg^{-1}) and Zn (304.1 mg·kg^{-1}) associated with the reducible fraction as listed in Table 2, posing serious threats that can be caused by dissolution of Fe–Mn oxy/hydroxides in highly acidic or reducing conditions (Fathollahzadeh et al., 2014). It should be highlighted that even though low F1 of Pb (9.34 mg·kg^{-1}), environmental and ecological risks cannot be eliminated since Pb in the reducible phase are potential mobility and might be released to the environment upon decomposition of the oxides under suboxic conditions and redox changes, and consequent bioavailability during dredging/remediation (Fathollahzadeh et al., 2014).

The oxidizable fraction (F3) is elemental speciations that bound to organic matter and sulfides. The results showed association as low as 4.9% and 9.59% for Pb and Zn, respectively (Fig. 8). Under oxidizing conditions, organic matter degradation can lead to a release of metals bound to this fraction. The small number of Pb (7.76 mg·kg^{-1}) and Zn (85.6 mg·kg^{-1}) associated with the oxidizable fraction as listed in Table 2, which released during the extraction is not bioavailable due to its association with stable humic substances that release small amounts of metals slowly (Fathollahzadeh et al., 2014). It can be presented that the potential risks posed by the oxidizable

fraction must be mainly considered in cases, while the soil exposed to oxidation environment.

The residual fraction (F4) is elemental speciation that existed in silicate lattices. Once the first three fractions were removed, the residual soil should contain mainly primary and secondary minerals. The results showed that Pb and Zn were associated with residual fraction 13.96% and 8.61% of their total concentrations, respectively (Fig. 8). The small number of Pb (22.1 mg·kg^{-1}) and Zn (76.9 mg·kg^{-1}) metals may be held within mineral crystal structure, and hard to be released in the solution over a reasonable time span under the conditions normally encountered in nature (Tessier et al., 1979).

It can be concluded that Pb and Zn had a small proportion of the residual fraction (13.96% and 8.61%) and relatively large proportion of the mobile fraction (F1+F2+F3) , indicating that two metals had a strong contribution from anthropogenic source in soils and a high probability transferring from soil to crops and underground water (Chai et al., 2015). It further indicated that the soil was contaminated by the lead-zinc tailing. It also implied that two metals had tremendous potential ecological risks to environment. In order to have a better understanding of the degree of risks posed by metals, the individual contamination factor (*ICF*) was introduced to estimate the relative retention time of metals in soil. The higher the *ICF* value is, the lower is the retention time and higher is the risk to the environment (Nemati et al., 2011; Zhao et al., 2012; Fathollahzadeh et al., 2014; Huang and Yuan, 2016) . The *ICF* value is obtained by dividing the concentrations of metals in the mobile fraction (F1+F2+F3) by the concentrations in residual fraction (F4) as *ICF* = (F1+F2+F3)/F4. Subsequently, *ICF* of Pb and Zn were calculated as 6.16 and 10.61, respectively. According to the reference (Huang and Yuan, 2016), if *ICF* of two metals > 6, they belonged to high contamination and consequently posed higher risks to the environment. Further, the contents of Pb and Zn available to plants during the growing season were determined by extraction with DTPA (Sánchez-Monedero et al., 2004; Chojnacka et al., 2005). The DTPA-available content of Pb and Zn in the contaminated soil were 39.9 and 170.7 mg·kg^{-1}. Plants in the cultivated land are directly affected by the available content of heavy metals (Zou et al., 2012). The available Pb and Zn are easy absorbed by the root and accumulated in crops, and the accumulated metals can be transferred into the food chain, with adverse consequences on human health.

Conclusions

The chemical composition, phase composition, thermal behavior of the lead-zinc tailing and contaminated soil from a lead-zinc mine in Hunan, China, were investigated by XRF, XRD, FTIR and TGA-DSC. The contents of Zn and Pb were 0.191 wt.% and 0.044 wt.%, respectively, for the lead-zinc tailing, while 0.190 wt.% and 0.031 wt.% for the contaminated soil. The main mineral phase in the lead-zinc tailing were quartz (78.3 wt.%), fluorite (6.1 wt.%), muscovite (5.2 wt.%), kaolinite

(5.3 wt.%) and franklinfurnaceite (5.1 wt.%), while the contaminated soil mainly consisted of quartz (77.2 wt.%), muscovite (8.1 wt.%), kaolinite (9.7 wt.%) and franklinfurnaceite (5.0 wt.%). The lead-zinc tailing and contaminated soil had a good thermal stability.

Furthermore, the petrography of lead-zinc tailing and chemical fractionations of Pb and Zn in the contaminated soil were studied in details. The mineral phases of lead-zinc tailing were galena, pyrite, chalcopyrite, sphalerite, quartz and fluorite. The mild acido-soluble (F1), reducible (F2), oxidizable (F3) and residual (F4) fractions for Pb were 5.90, 75.24, 4.90 and 13.96%, and for Zn were 47.74, 34.06, 9.59 and 8.61%, respectively. The individual contamination factor (*ICF*) of Pb and Zn were calculated as 6.16 and 10.61, respectively. The DTPA-available content of Pb and Zn in the contaminated soil were 39.9 and 170.7 mg·kg^{-1}. Thus, a large number of Pb and Zn was easy transferred from the contaminated soil to the food chain. The results can provide a base for selecting remediation strategies, as well as in-situ stabilization and phytoremediation could be the suitable candidates in the study area.

Acknowledgements

References

AKCIL, A., ERUST, C., OZDEMIROGLU, S., FONTI, V., BEOLCHINI, F., 2015, *A review of approaches and techniques used in aquatic contaminated sediments: metal removal and stabilization by chemical and biotechnological processes*, J. Clean. Prod., 86, 24-36.

ALI, H., KHAN, E., SAJAD, M. A., 2013, *Phytoremediation of heavy metals—Concepts and applications*, Chemosphere, 91, 869-881.

AMIN, N.-U., AHMAD, T., 2015, *Contamination of soil with heavy metals from industrial effluent and their translocation in green vegetables of Peshawar, Pakistan*, RSC Adv., 5, 14322-14329.

ANTONIJEVIC, M. M., DIMITRIJEVIC, M. D., MILIC, S. M., NUJKIC, M. M., 2012, *Metal concentrations in the soils and native plants surrounding the old flotation tailings pond of the Copper Mining and Smelting Complex Bor (Serbia)*, J. Environ. Monitor., 14, 866-877.

CHAI, Y., GUO, J., CHAI, S., CAI, J., XUE, L., ZHANG, Q., 2015, *Source identification of eight heavy metals in grassland soils by multivariate analysis from the Baicheng–Songyuan area, Jilin Province, Northeast China*, Chemosphere, 134, 67-75.

CHOJNACKA, K., CHOJNACKI, A., G RECKA, H., G RECKI, H., 2005, *Bioavailability of heavy metals from polluted soils to plants*, Sci. Total Environ., 337, 175-182.

CISZEWSKI, D., GRYGAR, T. M., 2016, *A Review of flood-related storage and remobilization of heavy metal pollutants in river systems*, Water Air Soil Poll., 227, 239.

FATHOLLAHZADEH, H., KACZALA, F., BHATNAGAR, A., HOGLAND, W., 2014, *Speciation of metals in contaminated sediments from Oskarshamn Harbor, Oskarshamn, Sweden*, Environ. Sci. Pollut. Res., 21, 2455-2464.

FLORIS, B., GALLONI, P., SABUZI, F., CONTE, V., 2017, *Metal systems as tools for soil remediation*, Inorg. Chim. Acta, 455, 429-445.

GAO, Y., GAO, Z., SUN, W., HU, Y., 2016a, *Selective flotation of scheelite from calcite: A novel reagent scheme*, Int. J. Miner. Process., 154, 10-15.

GAO, Z.-Y., SUN, W., HU, Y.-H., 2014, *Mineral cleavage nature and surface energy: Anisotropic surface broken bonds consideration*, T. Nonferr. Metal. Soc., 24, 2930-2937.

GAO, Z., GAO, Y., ZHU, Y., HU, Y., SUN, W., 2016b, *Selective flotation of calcite from fluorite: A novel reagent schedule*, Minerals, 6, 114.

GAO, Z., LI, C., SUN, W., HU, Y., 2017, *Anisotropic surface properties of calcite: A consideration of surface broken bonds*, Colloid. Surface. A., 520, 53-61.

GONZÁLEZ-VALDEZ, E., ALARCÓN, A., FERRERA-CERRATO, R., VEGA-CARRILLO, H. R., MALDONADO-VEGA, M., SALAS-LUÉVANO, M. Á., 2016, *Seed germination and seedling growth of five plant species for assessing potential strategies to stabilizing or recovering metals from mine tailings*, Water Air Soil Poll., 227, 24.

HU, P., YANG, H., 2013, *Insight into the physicochemical aspects of kaolins with different morphologies*, Appl. Clay Sci., 74, 58-65.

HUANG, H.-J., YUAN, X.-Z., 2016, *The migration and transformation behaviors of heavy metals during the hydrothermal treatment of sewage sludge*, Bioresource Technol., 200, 991-998.

LEI, M., TIE, B.-Q., SONG, Z.-G., LIAO, B.-H., LEPO, J., HUANG, Y.-Z., 2015, *Heavy metal pollution and potential health risk assessment of white rice around mine areas in Hunan Province, China*, Food Sec., 7, 45-54.

LI, C., FU, L., OUYANG, J., TANG, A., YANG, H., 2015, *Kaolinite stabilized paraffin composite phase change materials for thermal energy storage*, Appl. Clay Sci., 115, 212-220.

LI, C., OUYANG, J., YANG, H., 2013, *Novel sensible thermal storage material from natural minerals*, Phys. Chem. Minerals, 40, 681-689.

LINDSAY, W. L., NORVELL, W. A., 1978, *Development of a DTPA soil test for zinc, iron, manganese, and copper*, Soil Sci. Soc. Am. J., 42, 421-428.

MAHAR, A., WANG, P., ALI, A., AWASTHI, M. K., LAHORI, A. H., WANG, Q., LI, R., ZHANG, Z., 2016, *Challenges and opportunities in the phytoremediation of heavy metals contaminated soils: A review*, Ecotox. Environ. Safe., 126, 111-121.

MAO, X., JIANG, R., XIAO, W., YU, J., 2015, *Use of surfactants for the remediation of contaminated soils: A review*, J. Hazard. Materials, 285, 419-435.

NEMATI, K., BAKAR, N. K. A., ABAS, M. R., SOBHANZADEH, E., 2011, *Speciation of heavy metals by modified BCR sequential extraction procedure in different depths of sediments from Sungai Buloh, Selangor, Malaysia*, J. Hazard. Materials, 192, 402-410.

REN, L., LU, H., HE, L., ZHANG, Y., 2014, *Enhanced electrokinetic technologies with oxidization–reduction for organically-contaminated soil remediation*, Chem. Eng. J., 247, 111-124.

RUAN, H. D., FROST, R. L., KLOPROGGE, J. T., 2001, *The behavior of hydroxyl units of synthetic goethite and its dehydroxylated product hematite*, Spectrochim. Acta A., 57, 2575-2586.

S NCHEZ-MONEDERO, M. A., MONDINI, C., DE NOBILI, M., LEITA, L., ROIG, A., 2004, *Land application of biosolids. Soil response to different stabilization degree of the treated organic matter*, Waste Manage., 24, 325-332.

SHI, T., CHEN, Y., LIU, Y., WU, G., 2014, *Visible and near-infrared reflectance spectroscopy—An alternative for monitoring soil contamination by heavy metals*, J. Hazard. Materials, 265, 166-176.

SU, C., JIANG, L., ZHANG, W., 2014, *A review on heavy metal contamination in the soil worldwide: Situation, impact and remediation techniques*, Environ. Skeptics Critics, 3, 24-28.

TESSIER, A., CAMPBELL, P. G. C., BISSON, M., 1979, *Sequential extraction procedure for the speciation of particulate trace metals*, Anal. Chem., 51, 844-851.

VOLL, D., ANGERER, P., BERAN, A., SCHNEIDER, H., 2002, *A new assignment of IR vibrational modes in mullite*, Vib. Spectrosc., 30, 237-243.

WANG, J., GAO, Z., GAO, Y., HU, Y., SUN, W., 2016, *Flotation separation of scheelite from calcite using mixed cationic/anionic collectors*, Miner. Eng., 98, 261-263.

WANG, L., LIANG, T., 2015, *Geochemical fractions of rare earth elements in soil around a mine tailing in Baotou, China*, Sci. Rep., 5, 12483.

XU, S., SU, W., LIU, Y., JIANG, L., JI, S., OKAY, A. I., SENG R, A. M. C., 1992, *Diamond from the Dabie Shan metamorphic rocks and its implication for tectonic tetting*, Science, 256, 80-82.

YEUNG, A. T., GU, Y.-Y., 2011, *A review on techniques to enhance electrochemical remediation of contaminated soils*, J. Hazard. Mater., 195, 11-29.

ZHAO, S., FENG, C., YANG, Y., NIU, J., SHEN, Z., 2012, *Risk assessment of sedimentary metals in the Yangtze Estuary: New evidence of the relationships between two typical index methods*, J. Hazard. Mater., 241–242, 164-172.

ZHENG, Y.-X., LIU, W., QIN, W.-Q., HAN, J.-W., YANG, K., LUO, H.-L., 2015, *Selective reduction of $PbSO_4$ to PbS with carbon and flotation treatment of synthetic galena*, Physicochem. Probl. Miner. Process., 51, 535-546.

ZOU, T., LI, T., ZHANG, X., YU, H., HUANG, H., 2012, *Lead accumulation and phytostabilization potential of dominant plant species growing in a lead–zinc mine tailing*, Environ. Earth Sci., 65, 621-630.